NUREG/CR-1055
LA-8029-PR

Progress Report

MASTER

Criteria and Test Methods for Certifying Air-Purifying Respirators Against Radioiodine

October 1, 1976—September 30, 1978

University of California

LOS ALAMOS SCIENTIFIC LABORATORY
Post Office Box 1663 Los Alamos, New Mexico 87545

This is the first report in this series.

This report was not edited by the Technical Information staff.

NUREG/CR-1055
LA-8029-PR
Progress Report
RH

Criteria and Test Methods for Certifying Air-Purifying Respirators Against Radioiodine

October 1, 1976—September 30, 1978

Gerry O. Wood
Gerald J. Vogt
Douglas C. Gray
Claudine A. Kasunic

Manuscript submitted: August 1979
Date published: September 1979

Prepared for
Office of Nuclear Regulatory Research
US Nuclear Regulatory Commission
Washnigton, DC 20555

NRC FIN No. A7041

UNITED STATES
DEPARTMENT OF ENERGY
CONTRACT W-7405-ENG. 36

CRITERIA AND TEST METHODS FOR CERTIFYING AIR-PURIFYING RESPIRATORS AGAINST RADIOIODINE

Progress Report
October 1, 1976 - September 30, 1978

by

Gerry O. Wood
Gerald J. Vogt
Douglas C. Gray
Claudine A. Kasunic

ABSTRACT

A project has been initiated to provide a standard test procedure to define the effectiveness of air-purifying respirator cartridges or canisters for airborne radioiodine. The information, procedures, and apparatus designs will provide the means by which air-purifying respirators can be approved for this application. A considerable body of published and private information was surveyed to define the nature of the radioiodine challenge and the requirements of a respirator cartridge to protect against it. The critical parameters limiting the efficiency and capacity of a given adsorbent cartridge for a given vapor species are airflow rate, relative humidity, and vapor concentration. Cartridge or canister design parameters such as bed geometry and sorbent used are also critical. The extensive literature of radioiodine air cleaning was reviewed. This led to the conclusion that a respirator cartridge of high efficiency (protection factor of 1000) for recognized forms of airborne radioiodine was feasible. A preliminary test system was built. It was used to determine the magnitudes of effects of critical environmental and sorbent bed design parameters on the retention of methyl iodide. Potential radioiodine sorbents were challenged with parts-per-million concentrations of nonradioactive methyl iodide. The resulting breakthrough curves were best described by the equations of the Theory of Statistical Moments. Relative humidity, flow rate, bed diameter, and bed depth had the effects on bed capacity anticipated. However, a concentration effect on capacity was observed that has several implications for respirator cartridge lifetime predictions.

I. BACKGROUND

Irradiated fuel elements in nuclear reactors produce a variety of elements and their isotopes as by-products of fission. Radioactive iodine isotopes ^{131}I and ^{129}I may be significant health hazards due to the quantities produced, the specific activities, the half-lives, the volatilities of iodine compounds, the transfer of iodine through the food chain, and the physiological process of concentrating iodine in the thyroid. The nonradioactive (normal) iodine isotope ^{127}I is also formed in fuel elements and occurs naturally in air. Radioiodine formed in the atomic or ionic state can react to become airborne as stable molecules. It can also adsorb on particles or droplets and become airborne as aerosols.

The toxicity of radioiodine requires that concentrations of radioactive gases and aerosols in air should be limited. Under normal operating conditions such limitation of radioiodine in air within the work environment (containment area) and in air released to the external environment is accomplished by air cleaning through large high efficiency particulate air (HEPA) filters and adsorbent beds. Much research has been reported on optimizing and characterizing the performances of air cleaning filters and adsorbent beds for radioiodine. The ventilation and air cleaning facilities must also be designed to operate adequately even following a worst conceivable accident, such as an equipment failure, a spill, or a system upset. However, the air cleaning facilities, because of their size, may be remotely located from the source of radioactivity. And, it may be necessary for a worker to approach this source for maintenance or repair operations. In such cases, personal respiratory protection is required.

Three types of respiratory protection devices that could be (and have been) used for such applications are (1) supplied-air suits or facepieces, (2) self-contained breathing apparatuses, and (3) high-efficiency air-purifying filter respirators. Supplied-air devices can provide high protection factors (50-2000),[1] but also have several significant disadvantages. (1)They are limited in range of operation by the length of the air-supply hose. (2) The hose may interfere with work activities. (3) A reliable source of compressed and well-filtered air is required. Self-contained breathing apparatuses with full facepieces also can provide high protection factors (50-10 000) and have the advantage of portability, which allows their use in emergency situations. However, they are limited to short periods of use by the amount of air carried. They may otherwise interfere with work activities due to the weight and bulkiness of the air tanks. Full-facepiece, air-purifying respirators can provide protection factors of 50-500 when used with a high-efficiency filter or adsorbent bed and do not have the disadvantages listed for the other two kinds of protection.

Presently, Nuclear Regulatory Commission (NRC) guides limit the use of air-purifying respirators to protection against radioactive materials present as particulate aerosols, for which high-efficiency respirator filters have been shown to be effective.[2,3] While unapproved respirator canisters are manufactured to collect iodine vapors, NRC restricts their use due to (1) unknown collection efficiencies of sorbent cartridges for vapors of radioiodine compounds, (2) unknown length of time a cartridge will provide adequate protection, and (3) no odor warning of breakthrough. A test procedure and approval schedule is needed that will allow certification of respirator cartridges for this application. The Testing and Certification Branch (TCB) of the National Institute for Occupational Safety and Health (NIOSH) has indicated that they would adopt an approval schedule for certifying radioactive iodine air-purifying respirator cartridges, if a testing procedure detailing techniques and instrumentation were developed and the necessary regulations were promulgated by the NRC.

In the Industrial Hygiene Group of the Los Alamos Scientific Laboratory (LASL) we have accepted the responsibility of providing the NRC with information regarding the use of air-purifying respirators for protection against radioiodine ^{131}I.

II. APPROACH

To provide the guidelines needed by the NRC, literature surveys and professional contacts have been followed by test apparatus development and experimental studies of adsorption of iodine compounds. It was decided early in this project that, if possible, we would develop a test procedure for respirator cartridges using nonradioactive iodine compounds. The use of stable (^{127}I) iodine would be more acceptable to the NIOSH TCB and others. However, it raises the question of whether the adsorption behavior of normal iodine vapors is representative of the behavior of radioiodine vapors. This question must be experimentally resolved. The steps programmed to accomplish this project are:

1. Survey and analysis of the literature relating to air-purifying respirators, vapor adsorption, and radioiodine air cleaning. Contacts with professionals experienced in these fields.
2. Design and construction of an experimental apparatus for sorbent testing, including generation and detection systems for stable ^{127}I vapor species.
3. Experimental study of the adsorption of methyl iodide on a variety of potential respirator sorbents and examination of the effects of environmental and cartridge design parameters on this adsorption.
4. Experimental study of the adsorption of elemental iodine vapors under limited conditions, and further development of testing procedures.
5. Experimental study of the adsorption of hypoiodous acid (HOI) vapors, if it first can be shown that HOI can be generated at parts-per-million levels.
6. Design and construction of facilities for the use of radioiodine for sorbent testing and development of radioiodine generators and detectors.
7. Experimental study of the adsorption of iodine vapor species tagged with ^{131}I for comparisons of results with those obtained using stable ^{127}I species.
8. Development of final acceptance tests, apparatus, and criteria to be recommended to NRC for approval of respirator cartridges against radioiodine.
9. Publication of results of this project and transfer of the test procedures and techniques developed to the NIOSH TCB and assistance to them in the development of an approval schedule.

III. LITERATURE SURVEYS AND PROFESSIONAL CONTACTS

Literature surveys and professional contacts were made to obtain information upon which to base experimental studies and test procedures. Since very limited information was available on the performance of air-purifying respirator cartridges against radioiodine vapors, the extensive radioiodine air cleaning literature was examined in much detail. The expertise available here at LASL concerning the capabilities and limitations of respirators was supplemented with other sources and contacts. Visits of personnel involved in this project were made to the Oak Ridge National Laboratory, the Savannah River Plant of E. I. duPont, the NIOSH TCB in Morgantown, West Virginia, the NRC in Washington, D.C., the Fifteenth Department of Energy Nuclear Air Cleaning Conference, and the 1977 and 1978 American Industrial Hygiene Conferences. An abbreviated summary of some conclusions reached from the information thus accumulated follows. For simplicity, references to sources of information will be limited.

A. The Radioiodine Challenge

1. Reactor Iodine Isotope Production and Release. In the fission reaction, large atoms of uranium or plutonium are split into two or more smaller fragments plus a significant quantity of energy. The mass of each of the fragments formed is variable but the sum of the masses of all of the fragments plus the equivalent mass of the energy released must be equal to the mass of the original fissioning atom. Since the masses of the iodine isotopes are a little more than half of the mass of the fissionable isotopes, iodine is formed in significant quantities in fission reactors.

Three important factors to consider for each iodine isotope are the quantity formed, the radioactive half-life, and the specific activity (Table I).[4] Because of their retention in the reactor cladding and containment systems, the short half-life iodine isotopes are largely decayed out within the reactor and do not reach occupational exposure areas. The total production of all iodine isotopes in an operating reactor is on the order of 0.01 grams per megawatt-day of thermal power produced.[5] About 75% by weight of all of the iodine isotopes produced in an operating reactor is present in the form of the iodine-129 isotope.[5] This isotope is not considered an occupational hazard, due to its very low specific activity of 1.60×10^{-4} curies per gram, but its 17 million year half-life makes it a permanent environmental pollutant. Iodine-131 is considered a significant occupational health hazard. It has a specific activity of 1.24×10^{5} curies per gram and an 8.05 day half-life. This report will assume that all significant occupational exposures are due to iodine-131.

The fraction of iodine produced in reactor fuels, which is released to the occupational environment, has been measured and estimated under various conditions. Based upon this, 2-30% of the iodine is released under normal operating conditions and a maximum of 50% under maximum credible accident conditions. In reprocessing, where the spent fuel is cut into short lengths and dissolved in acid, up to 100% of the iodine present can be released. However, the total iodine activity present in the spent fuel is very much reduced by decay during the customarily long times between removing the fuel from use and reprocessing.

TABLE I

IODINE ISOTOPES IN NUCLEAR REACTORS

			Reactor Equilibrium		Occupational	
Iodine Isotope	Half-life	Specific Activity (Ci/g)	Activities[a] (kCi/MW)	Amounts (g/MW)	MPC_a (Ci/m^3)	(40 h/wk) (mg/m^3)
127	stable	—	—	b	—	1^c
129	$1.7x10^7$y	$1.60x10^{-4}$	---	b	$8x10^{-10}$	$5x1^{-3}$
131	8.05 d	$1.24x10^5$	24.6	0.20	$4x10^{-9}$	$3x10^{-11}$
132	2.3 h	$1.05x10^7$	36.9	0.0035	$1x10^{-7}$	$1x10^{-11}$
133	20.8 h	$1.16x10^6$	15.4	0.013	$2x10^{-8}$	$2x10^{-11}$
134	0.88 h	$2.70x10^7$	65.5	0.0024	$3x10^{-7}$	$1x10^{-11}$
135	6.7 h	$3.47x10^6$	51.3	0.015	$5x10^{-8}$	$1x10^{-11}$

---

[a] Reactor at equilibrium (>1 yr), no decay time, Ref. 4.

[b] Due to relative isotopic stability, the equilibrium amounts of these isotopes in a reactor are determined by leakage rates from the fuel elements.

[c] In the elemental form I_2.

2. Radioiodine Compounds in Air. Iodine is formed in the atomic state during the fission process. This atomic iodine is very reactive and quickly combines with other atoms and molecules in its environment to form a variety of more stable compounds. Articles in the literature show good agreement on the existence of three major radioiodine components present in the air around nuclear reactor fuels: inorganic iodine gases, organic iodine gases, and particulate iodine.

Molecules that have been identified among the inorganic iodine gases include diatomic iodine (I_2), hydrogen iodide (HI), HOI, and others present in much smaller quantities. I_2 results from the association of the iodine atoms produced with each other and is usually the predominant inorganic gaseous species in a dynamic system.[6] HI and HOI are formed by reactions of atomic iodine or I_2 with water and water vapor. I_2 and HI are relatively stable in air, but they have a strong tendency to condense and react on various surfaces. HOI decomposes in air at relative humidities less than about 80%.[6]

Approximately 90% of the organic iodine gas activity is due to methyl iodide,[7] with the rest of the activity divided among a variety of other compounds. These organic iodine gases are formed by reactions of inorganic iodine compounds with organic impurities present on surfaces, dissolved in reactor coolants, and present in the air in trace amounts. The high radiation exposure levels common around reactors tend to increase the proportion of organic iodine gases formed.[8]

Particulate forms of radioiodine result from the reactive binding of iodine and iodine compounds with existing particles and droplets, from adsorption of iodine gases on particles and droplets, and by primary particle formation due to atmospheric reactions or atomization of solutions containing dissolved radioiodine. For purposes or worker protection, the actual chemical compositions of particulate radioiodines are not important, since all can be removed by the use of HEPA filters.

From the preceding discussion, it is obvious that the forms in which radioiodine exists depend very much upon the materials and processes occurring in the work environment. Any potential respirator cartridge must be able to remove the variety of radioiodine forms that could be present.

3. Iodine Concentrations. Iodine ambient background concentrations are due to the stable isotope ^{127}I. This background can vary from time to time and from place to place, but average concentrations of 10^{-3} to 10^{-2} μg of I_2 per m^3 have been observed.[9] Ambient iodine exists in various molecular forms and can have a significant effect on the collection efficiency and capacity of an adsorbent used to remove radioiodine from the air. The stable iodine may occupy the available adsorption sites, displace adsorbed radioiodine, or participate in isotope exchange reactions with adsorbed radioiodine. Therefore, the ambient iodine must always be considered in the design of any radioiodine adsorption experiment or test.

The allowable concentration of radioiodine in a controlled area depends upon the maximum permissible concentration (MPC) to which an unprotected worker may be safely exposed and upon the degree of respiratory protection provided. Because the body efficiently concentrates all iodine in the thyroid gland, the MPC for iodine-131 must be set at very low levels. The current MPC for a 40-h work week, in a controlled area, is 9×10^{-9} $\mu Ci/cm^3$, or 7.2×10^{-8} $\mu g/m^3$ of I_2.[10] To put this MPC in perspective, consider that one part per billion (ppb) of I_2 by volume, at one atmosphere and 20°C, is 10.7 $\mu g/m^3$, or 8 orders of magnitude higher than the MPC. Put another way, the MPC corresponds to roughly 170 I_2 molecules/cm^3. The difficulty of measuring iodine concentrations in air at the MPC levels is obvious.

4. Respirator Cartridge Requirements. Ideally, the function of an air-purifying respirator is to clean the working atmosphere of ^{131}I to a level of one MPC or less, so that a person can work indefinitely for up to 40 h/wk. In actual use, a respirator may only extend the period during which a user can be exposed to a contaminated area before a maximum dose is accumulated. In either case, the protection factor received from an air-purifying respirator (PF_T) depends on the combination of facepiece fit (PF_F) and cartridge efficiency (PF_C): $1/PF_T = 1/PF_F + 1/PF_C$.

A comprehensive evaluation of the efficiencies of respirators as protection devices was published at LASL in 1976.[1] Recommendations were included for maximum protection factors (PF_Ts) of air-purifying respirators with high-efficiency ($PF_C \geq 3333$) particulate or vapor filters. When only a qualitative fit test is performed on the wearer, PF_Ts of 10 and 50 can be allowed for half-mask and full-facepiece air-purifying respirators, respectively. When an employer conducts quantitative respirator man tests on individual wearers in addition to establishing and enforcing a minimal acceptable respirator program, maximum PF_Ts of 50 and 500 are recommended for half-masks and full-facepieces, respectively. Since the assumed cartridge protection factor is much greater than the total protection factors ($PF_C \gg PF_T$), the total protection factor is nearly the same as that of the facepiece fit ($PF_T \cong PF_F$).

To make the respirator facepiece fit the limiting factor rather than the cartridge, a PF_C of at least 1000 is desirable. The maximum total protection would be $PF_T = 1/(1/500 + 1/1000) = 333$. Filter protection factors of at least 1000 are easily obtained for particulates of respirable sizes. It must be demonstrated that small adsorbent cartridges can provide such protection factors for gases and vapors of radioiodine.

B. Parameters Affecting Vapor Adsorption

1. Adsorbate Form. The mechanism and rate of vapor adsorption from air passing through an air-purifying bed can vary with the molecular species being adsorbed or reacted. Therefore, each molecular form of radioiodine in the challenge air must be considered in defining the capabilities of a respirator cartridge. Some molecular properties of iodine compounds which have been detected in nuclear environments are listed in Table II. Hydrogen iodide is included in this table, although it has not been considered a significant radioiodine form. These molecular properties can provide a hint as to relative adsorptivities and reactivities. For example, weaker (and longer) molecular bonds suggest greater ease of molecular dissociation and reaction with a substrate (I_2>HOI>CH_3I>HI); and lower boiling points suggest greater ease of condensation within porous structures for subsequent adsorption and/or reaction (I_2>CH_3I >HI).

2. Sorbent. The chemical and physical properties of the vapor collection medium, particularly those which critically affect adsorption, are often not known. Table III lists some of these properties. Attempts have been made, with limited success, to identify the properties important for filtration of radioiodine vapors from air. In a bed of fixed geometry the surface area is one of the

TABLE II

IODINE VAPOR SPECIES AND THEIR MOLECULAR PROPERTIES

Compound	Molecular Configuration	Iodine Bond Properties		Normal Boiling Point (°C)
		Strength (Kcal/mole)	Length (A°)	
Diatomic iodine	I-I	36.5	2.662	184.4
Hydrogen iodide	H-I	71.4	1.604	-35.4
Hypoiodous acid	H-O-I	56	2.0	decomposes
Methyl iodide	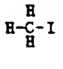 $H-\overset{H}{\underset{H}{C}}-I$	56	2.139	42.4

most significant parameters for adsorption since it is related to all the other physical properties listed in Table III. What happens once adsorption is achieved is determined by chemical properties of the surface.

The most widely used adsorption medium is activated charcoal because of its porosity and corresponding high surface area and its affinity for carbon atoms in organic molecules. Activated charcoal is also reactive with inorganic iodine to form about 56 kcal/mole C-I bonds. Activated charcoal is a relatively inexpensive sorbent. However, as a processed natural product, it has been found to vary widely in adsorption properties. This variation has been mainly due to variations in the source materials (coconut shells, coal, petroleum) which themselves are difficult to characterize. Each lot of activated charcoal must be tested to empirically determine its adsorption properties.

Chemically impregnated activated charcoals were developed for radioiodine vapors to obtain a more reproducible sorbent and to increase reactivity toward the less reactive forms, such as CH_3I. Triethylenediamine (TEDA), an amine of low volatility, has been used as an impregnant to react with and retain CH_3I. Potassium iodide (KI), sometimes with additional I_2, has been used to remove radioiodine by isotope exchange on the impregnated sorbent surface.

A third type of sorbent that has been used successfully for radioiodine vapors is silver exchanged zeolite or silver salt-impregnated alumina, silica gel, or other porous solid. Silver reacts readily with iodine to form a nonvolatile salt. Silver zeolites have been the most successful of these, but have found limited use in environmental air cleaning applications because of their cost. However, for a respirator cartridge, they may be cost effective. The silvered materials can be manufactured with reproducible properties, in contrast with activated charcoals. They are also not flammable.

3. Bed Geometry and Packing Density. The principal dimensions of a sorbent bed are depth and cross-sectional area and their product, the volume of sorbent. Sorption efficiency usually increases exponentially with bed depth. Linear flow velocity, an increase of which decreases sorption efficiency (see below), is inversely proportional to cross-sectional area. The limiting factor of pressure drop (breathing resistance) increases with bed depth and decreases with bed cross-section. Sorption efficiency and pressure drop both increase with bed packing density, which depends on granule shape, size, porosity, and even packing method. It is apparent that the design of an air-purifying respirator cartridge has an important effect on its performance. Optimizing the geometry and selecting the sorbent for maximum efficiency and minimum pressure drop is no trivial process. Typical charcoal respirator cartridges and canisters used for the removal of organic vapors have bed depths of 2.5-10 cm, cross-sectional areas of 30-400 cm^2, and weights of 50-1000 g.

TABLE III

CHEMICAL AND PHYSICAL PROPERTIES OF CHARCOALS
USED IN RADIOIODINE REMOVAL

Chemical Properties	Physical Properties
1. Moisture content	1. Particle grain size range
2. Type of impregnant	2. Surface area
3. Weight per cent of impregnant	3. Porosity
4. Sodium content	4. Particle grain density
5. Potassium content	5. Packing density
6. Iodine content	6. Pore distribution
7. Potassium/iodide ratio	7. Adsorption capacity
8. pH of water extract	
9. Susceptibility to poisoning or aging	

4. Face Velocity and Contact Time. The rate at which air moves through a sorbent filter bed also has a significant effect on adsorption efficiency. Face (or linear) velocity (V) is the ratio of volumetric airflow (w) through a bed to the cross-sectional area (A): $V = w/A$. Contact (or residence) time (t_c) is the average time that a molecule of air is within the bed volume of depth L. It is often approximated by $t_c = L/V$, which ignores the volume occupied by the solid sorbent particles.

Human breathing rates average from about 14 L/min to 75 L/min at sea level, depending on the work effort.[11] Ranges of face velocities for cartridges of 38- and 110-cm^2 cross section at these average flow rates are shown in Table IV. Since respiration is cyclical, instantaneous face velocities range considerably from the average. There is some evidence that adsorption capacities determined with average, constant airflows are representative of those obtained with cyclical flows.[12] However, high face velocities (>15 m/min) can significantly reduce adsorption efficiencies, particularly for shallow beds (<2.5 cm) and at high relative humidities.[13]

5. Challenge Concentration. Under certain circumstances the efficiency of a sorbent bed can be dependent on the concentration of contaminant vapor passed through the bed. Bed capacity and lifetime for removing a contaminant vapor are usually challenge concentration dependent. Efficiency is defined as $E = 1-(C_B/C_O)$, where C_B is the breakthrough concentration for a challenge concentration C_O. Decontamination factor (DF) or protection factor (PF) = $1/(1-E)$. For an idealized dynamic adsorption experiment, efficiency is a function of bed depth, linear flow velocity, adsorbent amount, slope of the linear adsorption isotherm, height of the mass transfer unit, and time, but not a function of adsorbate challenge concentration.[9] Efficiency can be a function of challenge concentration, however, if:[9,14]

a. The adsorption isotherm for the vapor/sorbent combination is nonlinear.

b. Other species in air, such as water vapor, interact with the vapor and/or sorbent.

c. A change of molecular form occurs, such as iodine reacting to form methyl iodide.

d. The adsorption bed is very inefficient due to improper design, packing, or selection of sorbent.

A continuous challenge of vapor to an adsorption bed will reduce efficiency with time. As sorbent granule capacity, a function of C_o, is reached at the front of the bed, the mass transfer zone will move down the bed. Capacity of the bed and the corresponding time at which that capacity is reached must be defined relative to a selected efficiency, DF, or breakthrough fraction. It is obvious that the higher the challenge concentration, the faster the sorbent and bed capacties will be reached. However, what is not so obvious is that other factors are involved in defining capacity and lifetime. For example, the magnitude of the sorbent capacity increases with the concentration of the vapor it is in equilibrium with. This is simply another expression of the adsorption isotherm.

TABLE IV

RANGES OF FACE VELOCITIES FOR AVERAGE VOLUMETRIC BREATHING RATES AND EXTREMES OF CARTRIDGE AND CANISTER CROSS-SECTIONAL AREAS

Average Breathing Rate (L/min)	Bed Cross Section (cm^2)	Face Velocity (cm/s)	Face Velocity (m/min)
14	38	6.1	3.7
	110	2.1	1.3
25	38	11.0	6.6
	110	3.8	2.3
50	38	21.9	13.2
	110	7.6	4.5
75	38	32.9	19.7
	110	11.4	6.8

Any consideration of the radioiodine challenge to a sorbent bed near the MPC ($7.2 \times 10^{-8}\ \mu g/m^3$ for ^{131}I) must take into account the ambient levels of total iodine in unfiltered air ($\geq 10^{-9}\ \mu g/m^3$). If the controlling mechanism of iodine removal from air is fixation by chemical reaction, the sorbent and bed capacity will be determined by the total iodine challenge concentration (ambient) rather than by the concentration of the radioiodine fraction. If the controlling mechanism of radioiodine from air is by isotope exchange, the background iodine (^{127}I) will not interfere in this process. However, in both cases the background iodine will interfere with the adsorption of radioiodine by occupying adsorption sites. Therefore, experiments or tests with challenge iodine concentrations below $10^{-8}\ \mu g/m^3$ probably are not representative of the performance of a test bed or respirator cartridge.

6. **Relative Humidity.** The effect of relative humidities above 70% for the air challenging a radioiodine sorbent is to significantly reduce adsorption efficiencies. This is particularly true for shallow beds of 2.5 cm or less. High humidity effects may be due to interaction of water vapor with the adsorbate and/or adsorbent or due to the displacement of adsorbed molecules by water vapor. If water vapor adsorption is significant,the heat of adsorption will raise the temperature of the sorbent, at least temporarily, which will reduce adsorption of other vapors.

The humidity to which a radioiodine respirator cartridge will be exposed will vary widely with time, place, and task. It will not necessarily be equilibrated at the ambient humidity before it is challenged with radioiodine. Another source of humidity in a respirator application is the users exhaled breath. The human breath is water saturated at about 37°C. As much as 1 g/min of water vapor is given off, enough to saturate 1000 L of air at 20°C. Therefore, the limitations imposed on adsorption efficiency by very high relative humidities must be considered.

7. **Temperature.** Air and adsorbent bed temperature can affect the mechanism and kinetics of adsorption, the relative humidity, and the volatility of certain impregnants. However, wide ranges of temperatures are usually necessary to change these significantly. The design of air cleaning filters must take into account the temperature increases that may occur due to high bed loadings of radioiodine after an accidental release. A respirator would probably be used at temperatures between 10 and 30°C (50 and 86°F). Therefore, temperature effects on respirator cartridge efficiency and capacity for radioiodine should be small compared to the effects of other parameters.

C. Air Cleaning Literature Reviews

A considerable amount of information has been published concerning the adsorption of vapors of radioiodine compounds in air cleaning applications. An extensive literature survey has been made as a foundation for this report and the experimental work that follows. A number of these reports were selected and reviewed as thorough studies representative of the body of literature on this subject.

Radioiodine ^{131}I is used in the typical efficiency test of a sorbent or sorbent filter used for air cleaning. Elemental iodine or methyl iodine is evaporated upstream of the bed in a dynamic system. Air samples are drawn through sampler beds (charcoal) upstream and downstream of the bed. Comparison of the amounts collected and measured by γ-counting techniques gives a direct measure of the bed efficiency. It cannot be assumed that the challenge and breakthrough concentrations are constant during the test. Only average concentrations can be calculated. An equilibration period (volume) may precede and/or a purge period may follow the test period.

1. Elemental Iodine Adsorption.[13,15-20] A majority of the experimental studies of I_2 adsorption on unimpregnated and impregnated activated charcoals suggests that decontamination factors greater than 1000 could be expected under the following conditions:

a. Bed depths ≥5 cm.
b. Face velocities ≤12 m/min.
c. Relative humidities up to 100%.
d. Challenge concentrations down to at least 10^{-2} $\mu g/m^3$ (background level of iodine).

Evidence was found for a more penetrating form of ^{131}I than the elemental iodine, either particulates or methyl iodide or hypoiodous acid. Charcoals that produced high pH (basic) when stirred in water were more efficient than those which produced low pH (acidic).

More limited data on the performance of silver zeolites (>99% exchanged) indicates that efficiencies better than those obtained with charcoals can be expected under the same conditions. In one case, a decontamination factor $>10^4$ was obtained for a 5-cm bed depth, 14 m/min face velocity, 100% relative humidity, and 4.7 mg/m^3 challenge concentration.

2. Methyl Iodide Adsorption.[13,19-25] Unimpregnated activated charcoals have been found to be inadequate for methyl iodine removal from air due to low capacities, particularly at high humidities. Therefore, potassium iodide (KI)- and TEDA-impregnated charcoals have been developed and used for radioiodine air cleaning. Optimum levels of impregnants are 0.5% KI or 5% TEDA. The latter has a higher capacity for methyl iodide, but only a slightly better adsorption efficiency. DFs greater than 1000 could be expected under the following conditions for the better KI- or TEDA-impregnated charcoals:

a. Bed depth. 5-10 cm.
b. Face velocities ≤12 m/min.
c. Relative humidities up to 100%,
d. Challenge concentrations ≥10 $\mu g/m^3$.

Under the same conditions only half as deep a bed is required for a 10^3 DF for elemental iodine. Silver zeolite under the same conditions provides methyl iodide removal approximately equivalent to that obtained with impregnated charcoals.

3. Hypoiodous Acid Adsorption.[26] Activated charcoal impregnated with TEDA (5%) is slightly better for adsorbing radioiodine in the form of HOI than when impregnated with KI (5%). Extrapolation of absorption efficiencies for 1- to 6-cm bed depths indicates that a DF of at least 1000 can be achieved for this species within the following limits:

a. Bed depths ≥10 cm.
b. Face velocities ≤13 m/min.
c. Relative humidities up to 100%.
d. Challenge HOI concentrations near 10^{-5} $\mu g/m^3$.

Under equivalent conditions 10-cm deep beds of unimpregnated activated charcoal or silver zeolite can provide DFs of approximately 100. Limited experiments at a lower concentration of 10^{-6} $\mu g/m^3$ HOI and 60% relative humidity showed greater bed penetrations for the impregnated charcoals. However, this apparent concentration effect was not supported by other data that gave linear log (% HOI penetration) vs bed depth plots. In all cases some desorption of ^{131}I with continued air purging after loading was observed; but the form of the desorbed ^{131}I was probably not HOI, but I_2 or organic iodide.

4. Conclusions. The available information on sorbents for radioiodine vapors indicates that a respirator cartridge with protection factor of 1000 can be designed. A cartridge with a currently available TEDA- or KI-impregnated charcoal or silver zeolite would need to be rather large, 10-cm deep and 62 cm^2 cross section, to assure protection factors of 1000 for all species. However, reasonable efforts at sorbent development and cartridge design should be able to reduce these dimensions. Alternate options are (1) to reduce the requirements on a cartridge for example, to a protection factor of 200; or (2) to limit the situations in which an air-purifying respirator could be used, for example, to moderate humidity or light work load situations. In addition to the sorbent, a respirator cartridge for radioiodine should have a HEPA filter at the bed inlet to remove particulates that may contain radioiodine. A second HEPA filter at the bed outlet may also be advisable to remove fines generated from the sorbent.

There appears to be no reliable evidence for a dependence of sorbent efficiency on challenge vapor concentration for efficient beds. Such an effect would be due to nonlinearity of the adsorption isotherm at low concentrations. Nonideal conditions, such as high humidity or iodine-surface reactions or poor sorbent efficiency, can give apparent concentration effects.

A radioiodine respirator cartridge test should look for an apparent concentration effect. A range of challenge concentrations should be used. The most stable and penetrating iodine vapor species, CH_3I, should be used. However, each type of sorbent should also be tested with I_2 and HOI to confirm that CH_3I is indeed the most penetrating form. Extreme conditions of nearly 100% relative humidity and 75 L/min airflow should be used unless more limited ranges of application are specified.

D. Radioiodine Respirator Literature[27]

One report has been published describing results of testing respirator canisters for protection against radioiodine. All tests were done with ^{131}I-labelled CH_3I. Three cartridges, 2.5-cm deep and 10-cm diam, were tested at 64 L/min (8.15 m/min), 50% relative humidity, and 32°C. DFs of 3.3, 4.0, and 5000 were obtained. Performance of the second cartridge improved to DF = 1430 at 33 L/min, 50% relative humidity and to DF = 13 at 33 L/min, 93% relative humidity. The third tested cartridge had a TEDA-impregnated charcoal. It continued to give DFs $\geq$5000 at 93% relative humidity and $\geq$30 after aging and poisoning tests.

These limited results confirm that it is possible to prepare a radioiodine respirator cartridge with a DF $\geq$1000 at conditions approaching the extremes of breathing rate and relative humidity. The question of how much performance will change with time of use (aging) remains to be resolved. The test procedure this program is to develop will help answer this question.

IV. EXPERIMENTAL

A sorbent test system was built for the generation, adsorption, and detection of vapors of methyl iodide in air at parts-per-million concentrations. Figure 1 is a schematic of this system. The carrier air preparation section is pictured in Fig. 2, and the vapor generation and test section is shown in Fig. 3. Pressurized air was regulated, filtered, and humidified to obtain the conditions desired. A calibrated electronic flow meter and an electronic humidity meter were used to monitor, and in the case of the latter, to control these conditions. Liquid methyl iodide was metered at a calibrated rate by a syringe pump into a heated port. There it vaporized and was swept into the main airstream by an auxiliary (0.2 L/min) airstream. From this point in the apparatus to the sorbent bed, all tubing was 2.4-cm-i.d. glass. An air monitor with a photoionization detector was used to monitor the output of the syringe pump generation system. Air entering the charcoal bed and effluent air were alternately sampled by an automated gas sampling valve with Teflon loops. Such samples were introduced into a gas chromatograph, separated on a silicone OV-7 (15% on 100/120-mesh Chromosorb G) column (4-mm i.d. x 1.8-m long, 100°C, 20 cm^3/min 19:1 Ar/CH_4) and measured for methyl iodide with a Ni-63 linearized electron capture detector. An electronic peak integrator was used to quantitate the methyl iodide peaks and to

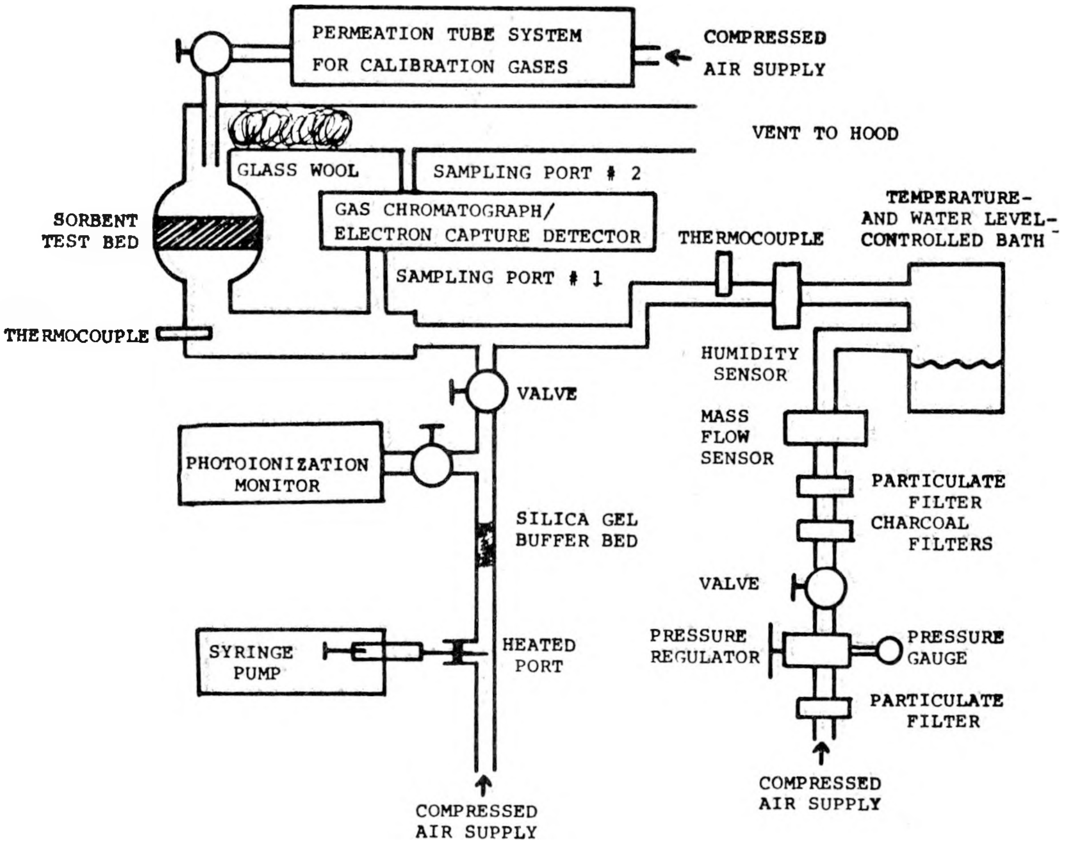

Fig. 1.

Schematic of the preliminary sorbent test system using methyl iodide vapors.

record elapsed times. Teflon and glass were used throughout the sampling and analysis system except for the sampling valve, which was Hastalloy C, and the detector, which was stainless steel (300°C).

The valve/gas chromatograph/electron capture measuring system was frequently calibrated using Teflon permeation tubes containing liquid methyl iodide. The outputs of these permeation tubes, maintained at constant temperatures (±0.3°C), were quite constant over periods of many months, as determined by weekly weighings. These known methyl iodide outputs were mixed in known airflows to produce known methyl iodide concentrations (0.03-26 ppm). Calibration indicated that the detector response was indeed linear over at least 3 orders of magnitude and methyl iodide concentration was proportional to measured peak area. The response of the measurement system was affected slightly by relative humidity of the air. The limit of measurement was about two parts-per-billion methyl iodide in air.

The experimental procedure was as follows. The airflow (20-40 L/min) was stabilized at a selected relative humidity. The syringe pump was started and its output was diverted to the photoionization monitor. Meanwhile, the output of a calibrated permeation tube was introduced at 1 L/min into the main airstream. The detector system was recalibrated in this way. The flow from the permeation tube to the main airstream was stopped. A charcoal bed was prepared by weight in a cylindrical glass tube of selected diameter. This was placed in the flow system. After 5 min, the syringe pump output was diverted into the main airstream and the experiment was begun. After significant breakthrough (10-20%) of the test bed had occurred, the experiment was terminated.

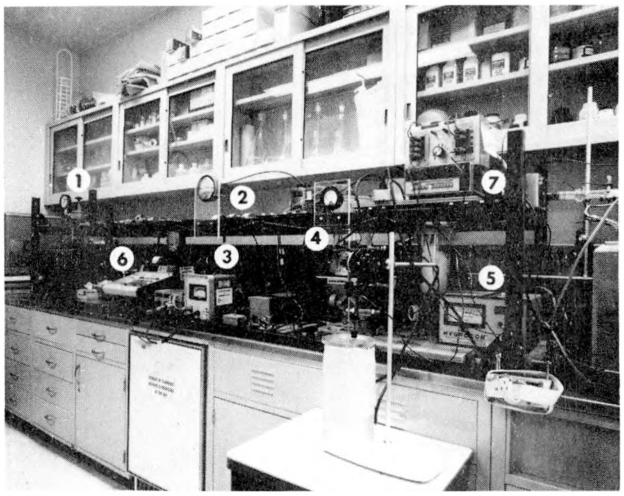

Fig. 2.
Carrier air preparation section of the test system: (1) Airflow regulator, (2) air purification filters, (3) electronic airflow monitor, (4) humidification chamber, (5) relative humidity indicator and controller, (6) data acquisition and calculation unit, and (7) temperature monitor.

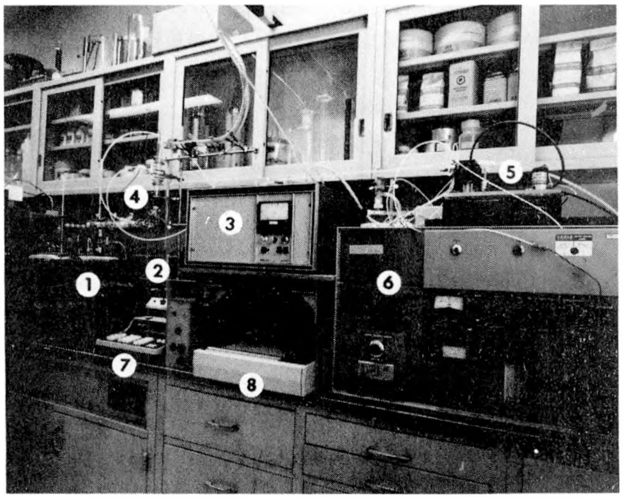

Fig. 3.
Vapor generation and test sections: (1) elemental iodine sublimation chamber, (2) syringe pump for methyl iodide vapor generation, (3) photoionization monitor for challenge vapor, (4) charcoal test bed, (5) automated air sampling valve, (6) GC with electron capture detector, (7) chromatograhic peak integrator, and (8) strip chart recorder.

V. METHYL IODIDE STUDIES AT PARTS-PER-MILLION LEVELS

A. Breakthrough Curves

Sorbent bed breakthrough data was first accumulated and analyzed for methyl iodide in air at parts-per-million challenge concentrations. The raw data obtained using the flow system of Figs. 1-3 were in the form of gas chromatograph (GC) peak areas vs elapsed time, t. Syringe pump output and volumetric airflow rates were used to calculate challenge concentration C. GC calibration factors obtained from permeation tube outputs were used to convert peak areas to breakthrough concentrations C_B. One example of a breakthrough curve of fractional breakthrough, C_B/C_o, vs t is shown in Fig. 4 from an experiment with 5% TEDA-impregnated Barnebey Cheney charcoal. The conditions were:

25.7 ppm (117 mg/m^3) challenge concentration
50% relative humidity
15.1 m/min face velocity (20 L/min)
4.1-cm-diam x 2.5-cm-deep bed

Experiments were seldom continued much beyond $C_B/C_o = 0.1$, but in this case extended over nearly 3 orders of magnitude from 2.72×10^{-4} at 2 min to 0.218 at 358 min.

The first objective in analyzing the CH_3I breakthrough data was to determine the mathematical form of the breakthrough curves. Several models that have been proposed were tested against the data in Fig. 4. The most common descriptions of breakthrough curves are based on the Mecklenburg equation

$$t_B = \frac{a_1}{C_o} (b_1 - h) \; , \tag{1}$$

where h is the "dead layer" depth or the "critical" bed depth, i.e., that value below which breakthrough would be instantaneous. In this equation and those following a_i and b_i refer to combinations of parameters that are constant for a given breakthrough curve. The many variations of the Mecklenburg equation that have been proposed have differed primarily in the expression used to calculate h. For example, the Klotz, Sillen, Van Dongen, Wheeler, and Jonas equations have $h = -a_2 \ln (C_B/C_o)$. The Danby equation has $h = -a_3 \ln [C_B/C_o - C_B)]$, which is equivalent in form to the others for $C_B/C_o < 0.1$. All these variations of the Mecklenburg equation predict that a plot of t_B vs $\ln (C_B/C_o)$ or vs $\log (C_B/C_o)$ would be linear. Figure 5 shows such a plot for the breakthrough data under consideration. This plot is clearly nonlinear over the entire range of data. Therefore, the variations of the Mecklenburg equation with $h = -a_2 \ln (C_B/C_o)$ do not adequately describe the breakthrough of methyl iodide in this experiment.

The second description attempted for methyl iodide breakthrough was an empirical relationship,

$$t_b = a_4 (C_B/C_o)^{b_4} \tag{2}$$

This implies that a plot of $\log t_B$ vs $\log (C_B/C_o)$ is linear. Such a plot (Fig. 6) for the same set of data was linear only in the range $C_B/C_o = 0.005$ to 0.22 and, therefore Eq. (2) is not adequate. Furthermore, the parameters from such a data fit have no known physical significance.

The most successful fit of this set of breakthrough data was obtained using the equations developed for a Theory of Statistical Moments by Otto Grubner and Dwight Underhill.[28] By this theory the breakthrough curve can be generated from its moments by a series such as the Gram-Charlier series. Simplifications of the adsorption mechanism are required to obtain analytically useful equations whose parameters are related to parameters of physical significance. The reference cited provides further explanation. A basic equation obtained by retaining the first three statistical moments (m_1, m_2, m_3) is

$$t_B = m_1 + \sqrt{m_2}\, X_B + \frac{m_3}{6m_2} (X_B^2 - 1), \tag{3}$$

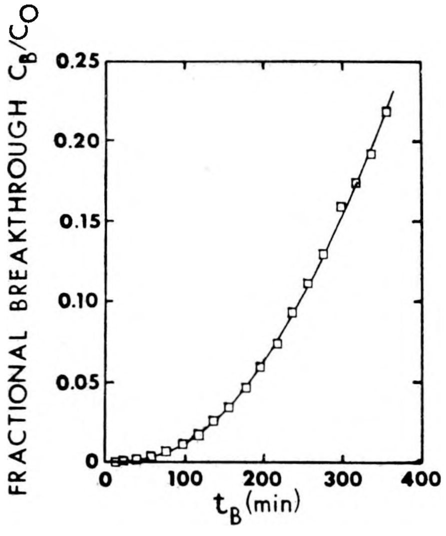

Fig. 4.
Breakthrough curve for methyl iodide penetrating a bed of 5% TEDA impregnated Barnebey Cheney 487 charcoal. Conditions are cited in the text.

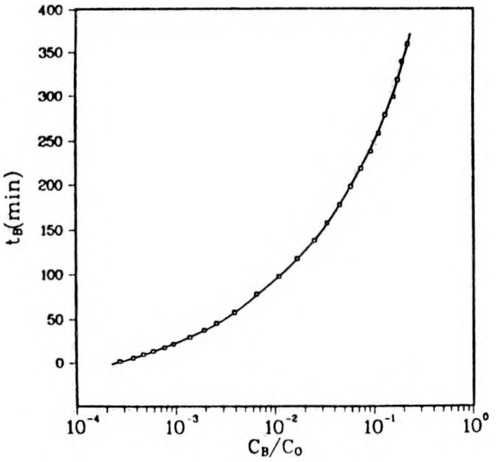

Fig. 5.
Semilog plot of data from the breakthrough curve of Fig. 4.

where

$$C_B/C_o = \frac{1}{\sqrt{2\pi}} \int_{-\infty}^{X_B} \exp\left[\frac{-X^2}{2}\right] dx. \tag{4}$$

Equation (4) is the normal probability integral or error function whose values of X_B for C_B/C_o are readily available in tabulated form or may be calculated on a programmable calculator. Equation (3) predicts a parabolic relationship between t_B and X_B for three statistical moments and a linear relationship if two statistical moments are sufficient. Figure 7 shows a plot of t_B vs X_B for the same set of data considered previously. This plot is linear only for $X_B > -1$ or $C_B/C_o > 0.16$. However, a parabolic fit of the data by least-squares regression to $t_B = a_o + a_1 X_B + a_2 X_B^2$ produced a curve such as that drawn through the data points. Such a fit is excellent over the entire range of the data with $m_1 = 578$ min, $\sqrt{m_2} = 274$ min, and $m_3/6m_2 = 34.36$ min. Another way to check the parabolic form of the t_B vs X_B plot is to graph $(t_B - m_1 - m_3/6m_2)/X_B$ vs X_B, as in Fig. 8. The linearity of this graph with a correlation coefficient of $r^2 = 0.9975$ is a confirmation of the data fit.

Fits of the parabolic form of the Theory of Statistical Moments to breakthrough curves for two other charcoals are shown in Fig. 9. The circles represent data for a bed of Union Carbide ACC nonimpregnated charcoal and the squares represent data for a bed of North American Carbon G615 KI/TEDA-impregnated charcoal. Experimental conditions were:

25.7 ppm (117 mg/m^3) challenge concentration
33% relative humidity
5.3 m/min face velocity (20 L/min)
6.9-cm-diam x 2.5-cm-deep bed

Again, the theory fit the breakthrough data very well for these different types of charcoal. It is interesting to note that the t_B vs X_B curve for the NAC G615 charcoal is linear for $-1 > X_B > -3.09$ $(0.16 > C_B/C_o > 0.001)$. In this linear region the simplified Theory of Statistical Moments with two, rather than three, moments can be used to describe the data: $t_B = m_1 + \sqrt{m_2}\, X_B$.

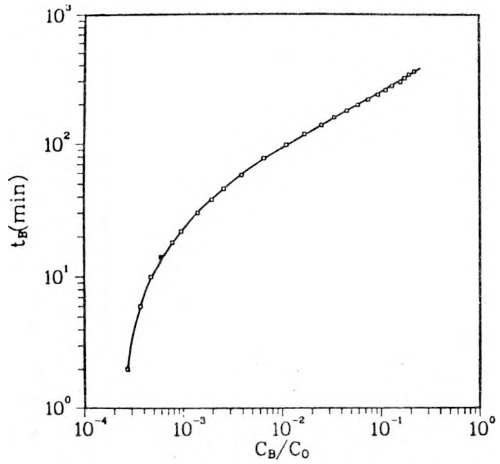

Fig. 6.
Log-log plot of data from the breakthrough curve of Fig. 4.

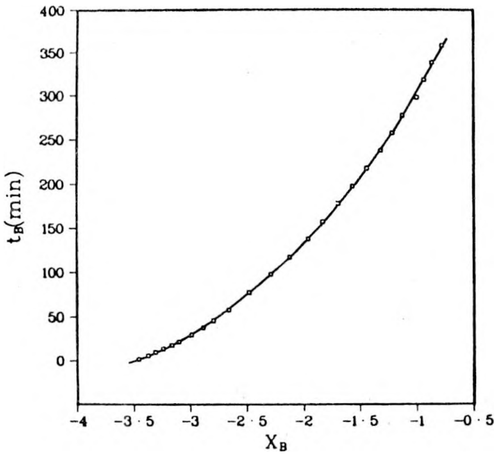

Fig. 7.
Probability plot of data from the breakthrough curve of Fig. 4. Solid line is calculated from a least-squares fit of data to Eq. (3).

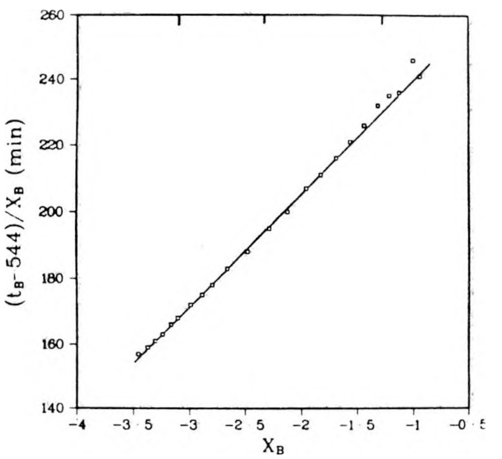

Fig. 8.
Graphical test of the least-squares fit of data from the breakthrough curve of Fig. 4 to the parabolic equation [Eq. (3)].

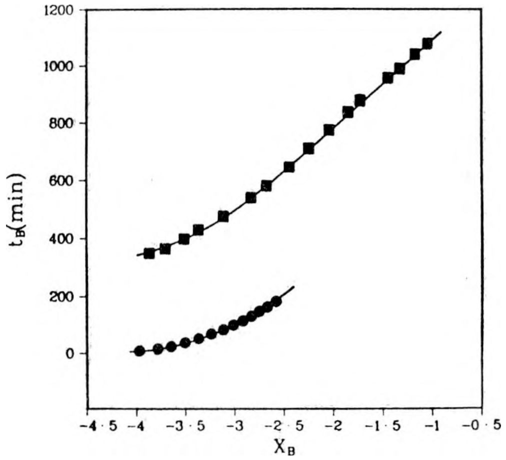

Fig. 9.
Probability plots of breakthrough curve data: ■ , a KI/TEDA-impregnated charcoal (NAC G615); and ●, a nonimpregnated charcoal (UC ACC).

Breakthrough curves were obtained for six activated charcoals and four impregnated charcoals of the type used in radioiodine air cleaning applications. The conditions were the same as in the preceding paragraph. These sets of data were fit to the statistical moments equations to give the parameters listed in Table V. Breakthrough times corresponding to protection factors (DFs) of 10, 100, and 1000 are also listed in Table V. Reproducibility of these early experiments is shown by the four replicate experiments with Union Carbide ACC charcoal. Within this reproducibility, the nonimpregnated adsorbents were similar in performance. The impregnated sorbents were much better for methyl iodide retention. The order of results shown in Table V was not surprising. However, this does demonstrate one use of breakthrough curve fitting by statistical moments.

Another series of CH_3I breakthrough measurements compared the performances of several types of potential radioiodine sorbents. These experiments were done using a calibrated permeation tube as the CH_3I source and a photoionization detector to determine breakthrough. Experimental conditions were:

8.96 ppm (40.4 mg/m^3) challenge concentration
50% relative humidity
5.4 m/min face velocity (0.27 L/min)
0.8-cm-diam x 2.5-cm-deep bed

Figures 10 and 11 show the results of these experiments as plots of t_B vs X_B. Duplicate runs were made with all but the silver zeolite. Over the range $-1.28 > X_B > -3.09$ ($0.1 > C_B/C_o > 0.001$) these graphs were apparently linear.

The data were fit by the simplified Theory of Statistical Moments to give the parameters m_1 and $\sqrt{m_2}$ in Table VI. A third parameter to account for nonlinearity of t_B vs X_B below $X_B = -3.09$ ($C_B/C_o = 0.001$) might have been required if the detector had been sensitive enough to measure in this region. A quantity called the measure of performance,[29] $MP = m_1/\sqrt{m_2}$, is also given in Table VI. A comparison of these values shows that the order of CH_3I retention capacity was silver zeolite ≫BC-487 (5% TEDA), >NAC-G615 (KI, TEDA), UC-ACC (unimpregnated)>SS-633 (5% KI_3)> BC-727 (5% KI_3). The latter two had lower capacities for normal methyl iodide removal, because they already had significant amounts of normal iodine present. The KI_3 ($KI + I_2$) impregnant is added to bind adsorbed radioiodine by isotope exchange reactions.

TABLE V

BREAKTHROUGH CURVE PARAMETERS AND BREAKTHROUGH TIMES FOR METHYL IODIDE AND SEVERAL CHARCOALS

Sorbent			Calculated Parameters (min)			Breakthrough Times (min) For Protection Factors		
Source	Designation	Impregnant	m_1	$\sqrt{m_2}$	$m_3/6m_2$	10	100	1000
Union Carbide	ACC	None	1005	417	43.6	499	228	88
			1268	571	67.9	580	241	85
			1179	458	45.2	621	314	149
			1501	675	80.2	688	286	101
Westvaco	WV-H	None	1034	473	58.2	466	192	70
Witco	337	None	1017	416	43.7	512	243	105
Pittsburgh AC	BPL	None	1239	493	49.5	640	312	139
Narbada	NG	None	1619	727	88.1	744	318	125
Fisher	5-685-B	None	1374	585	65.4	667	304	126
North American Carbon	G-618	TEDA	3295	1240	123.4	1786	958	517
	G-615	KI/TEDA	1533	429	32.7	1005	682	488
Barnebey Cheney	487	TEDA	2480	800	62.4	1497	899	543
Sutcliffe-Speakman	208C	TEDA	2923	983	94.2	1725	1055	691

B. Effects of Parameters on Breakthrough Times

1. Challenge Concentration

Breakthrough curves were obtained for two charcoals to study effects of challenge vapor concentrations on breakthrough times. The first series used Union Carbide ACC unimpregnated charcoal at these experimental conditions:

0.90 to 25.7 ppm (4.0 to 117 mg/m^3) challenge concentration
33% relative humidity
5.3 m/min face velocity (20 L/min)
6.9-cm-diam x 2.5-cm-deep bed

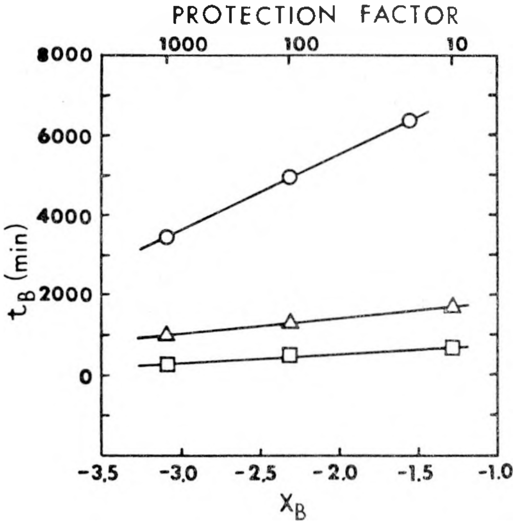

Fig. 10.
Probability plots of breakthrough curve data obtained for 8.96 ppm methyl iodide. Conditions are cited in the text. ○ , *silver zeolite;* △, *5% TEDA-impregnated Barnebey Cheney 487 charcoal;* □, *KI/TEDA-impregnated North American Carbon G-615 charcoal.*

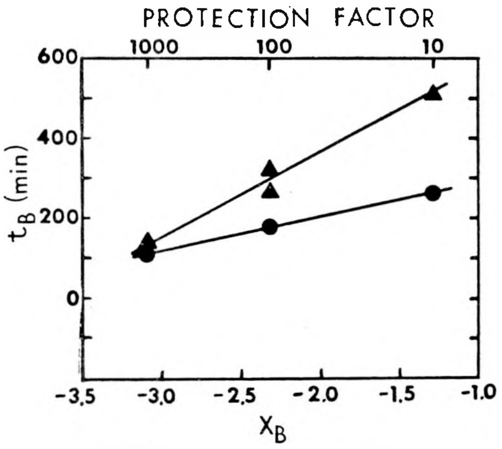

Fig. 11.
Probability plots of breakthrough curve data obtained for 8.96 ppm methyl iodide. Conditions are cited in the text ●, *5%* KI_3-*impregnated Sutcliffe Speakman 633-charcoal and 5%* KI_3-*impregnated Barnebey Cheney 727 charcoal;* ▲, *nonimpregnated Union Carbide ACC charcoal.*

TABLE VI

BREAKTHROUGH CURVE PARAMETERS, MEASURED BREAKTHOUGH TIMES, AND MEASURES OF PERFORMANCE FOR METHYL IODIDE AND SEVERAL SORBENTS

Sorbent	Parameters		Breakthrough Times (min)			Measure of Performance[a]
	m_1	$\sqrt{m_2}$	PF=10	PF=100	PF=1000	
Coast Engineering Lab Silver Zeolite	9378	1908	6380[b]	5000	3450	4.91
Barnebey Cheney 487	2284	441	1730	1230	936	5.18
(5% TEDA)	2117	357		1285	1020	5.93
North American Carbon	915	205	637	474	260	4.46
GG15 (KI,TEDA)	968	216	669	515	270	4.48
Union Carbide ACC	812	215	532	324	142	3.78
(Unimpregnated)	758	205	501	267	132	3.70
Sutcliffe Speakman 633	407	94	286	191	116	4.34
($5\%\ KI_3$)	339	76	241	164	104	4.48
Barnebey Cheney 727	344	74	249	172	115	4.65
($5\%\ KI_3$)	355	71	264	190	136	5.00

---

[a] MP = $m_1/\sqrt{m_2}$, Ref. 29.

[b] PF = 16.7.

Results are plotted in Fig. 12 as log t_B vs log C_o for protection factors of 10, 100, and 1000. Since these plots were apparently linear, the following relationships were calculated by linear least-squares fitting:

PF = 10, $t_B = (94 \pm 81)\ C_o^{-0.17 \pm 0.03}$
PF = 100, $t_B = (390 \pm 38)\ C_o^{-0.15 \pm 0.04}$
PF = 1000, $t_B = (180 \pm 32)\ C_o^{-0.19 \pm 0.07}$

The ± values refer to standard deviations calculated for 11 experimental points. The relative values of these standard deviations confirm that the dependence of protection factors on challenge concentration is real.

A similar series set of experiments was done with Barnebey Cheney 487 TEDA (5%)-impregnated charcoal at challenge methyl iodide concentrations from 0.87 to 29.0 ppm. Other conditions were:

30.3 m/min face velocity (40 L/min)
50% relative humidity
4.1-cm-diam x 2.5-cm-deep bed

Breakthrough times for protection factors of 2, 10, and 100 (penetration fractions of 0.5, 0.1, and 0.01) were plotted in Fig. 13 as log t_B vs log C_o. Reproducibility was much improved for these experiments as seen by the overlapping of duplicate points at 12.1, 20.6, and 29.0 ppm. Again, these plots were apparently linear with the results:

PF = 2, $t_B = (6750 \pm 570)C_o^{-1.06 \pm 0.06}$, $r^2 = 0.996$
PF = 10, $t_B = (2310 \pm 110)C_o^{-1.01 \pm 0.03}$, $r^2 = 0.999$
PF = 100, $t_B = (230 \pm 16)C_o^{-0.73 \pm 0.09}$, $r^2 = 0.994$

and, again, a significant challenge concentration effect was observed.

2. Relative Humidity. Variations of breakthrough times with relative humidity were also studied for the Barnebey Cheney 487 charcoal under these conditions:

25.7 ppm (117 mg/m^3) challenge concentration
33-100% relative humidity
15.1 m/min face velocity (20 L/min)
4.1-cm-diam x 2.5-cm-deep bed

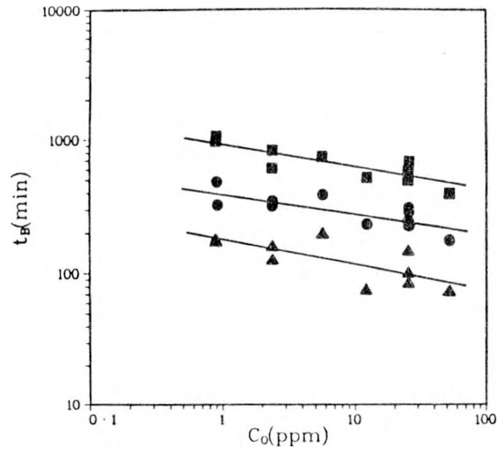

Fig. 12.
Challenge concentration dependence of breakthrough times for methyl iodide and non-impregnated Union Carbide ACC charcoal at protection factors: 2, ▲, and 10, ■ , and 100, ●, and 1000, ▲.

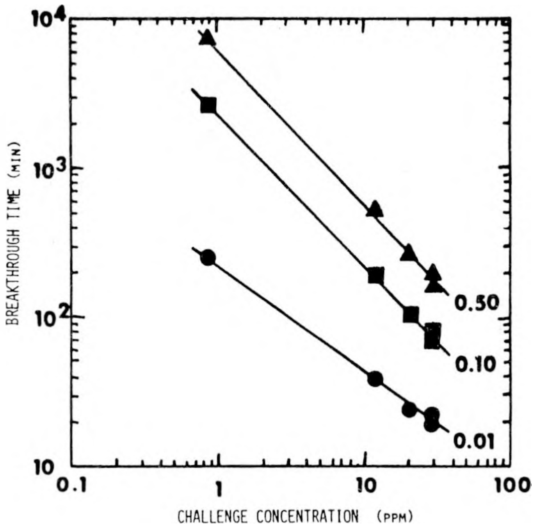

Fig. 13.
Challenge concentration dependence of breakthrough times for methyl iodide and 5% TEDA-impregnated Barnebey Cheney charcoal at protection factors: 10, ■ , and 100, ●.

The log t_B vs log (%RH) plots in Fig. 14 show apparent linear relationships which give:

PF = 10, $t_B = 9350\,(\%\mathrm{RH})^{-0.93}$, $r^2 = 0.951$
PF = 100, $t_B = 6640\,(\%\mathrm{RH})^{-1.05}$, $r^2 = 0.903$
PF = 1000, $t_B = 8589\,(\%\mathrm{RH})^{-1.40}$, $r^2 = 0.764$

The r^2 values are linear correlation coefficients for log-log plots. A second set of experiments varying relative humidity for BC-487 and UC-ACC charcoals at a higher face velocity of 48 m/min (63.5 L/min) with other conditions the same gave for PF = 10:

BC-487, $t_B = 10906\,(\%\mathrm{RH})^{-1.33}$, $r^2 = 0.958$
UC-ACC, $t_B = 6318\,(\%\mathrm{RH})^{-1.50}$, $r^2 = 0.956$

These experiments confirm the expected result that breakthrough times for a given protection factor decrease with increasing relative humidity. Our experiments indicate that this decrease can be approximated by a power equation. For the TEDA-impregnated BC-487 charcoal the negative exponent of the power equation increased only slightly for a more than threefold change in face velocity or for a 1000-fold change in protection factor.

3. Flow Rate. Effects of volumetric flow rate on the breakthrough times of methyl iodide were further studied with BC-487 charcoal under these conditions:

25.7 ppm (117 mg/m^3) challenge concentrations
50% relative humidity
(4.9-14.7) m/min face velocity (10-30 L/min)
5.1-cm-diam x 2.5-cm-deep bed

Figure 15 shows log-log plots of the t_B vs flow rate data obtained for three protection factors. These plots are also linear, yielding the power equations:

PF = 10, $t_B = 9629\,V^{-1.33}$, $r^2 = 0.988$
PF = 100, $t_B = 9292\,V^{-1.64}$, $r^2 = 0.986$
PF = 1000, $t_B = 11229\,V^{-2.10}$, $r^2 = 0.956$

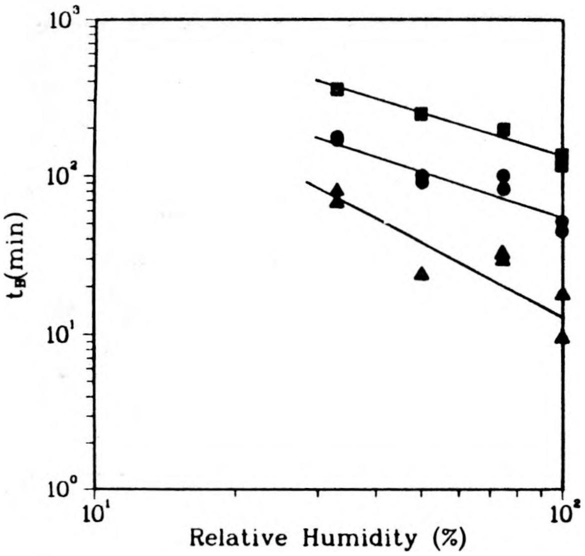

Fig. 14.
Relative humidity effects on breakthrough times for methyl iodide and 5% TEDA-impregnated Barnebey Cheney charcoal at protection factors: 10, ■ *, and 100,* ●*, and 1000,* ▲.

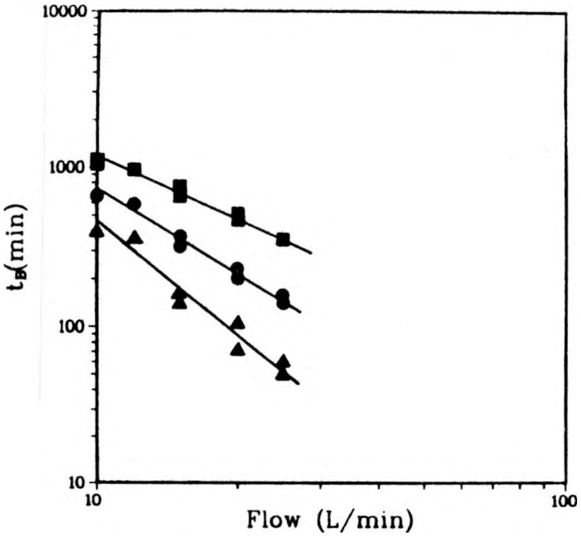

Fig. 15.
Flow rate effects on breakthrough times for methyl iodide and 5% TEDA-impregnated Barnebey Cheney charcoal at protection factors: 10, ■ *, and 100,* ●*, and 1000,* ▲.

V is the linear velocity (m/min) corresponding to flow rate in Fig. 15. The negative coefficients of the power expressions increase significantly with orders of magnitude increases in protection factors.

4. Bed Diameter. Linear velocity can be reduced for a fixed volumetric flow rate by increasing the bed diameter. This also increases the bed capacity for a fixed bed depth by increasing the amount of sorbent. Figure 16 shows the results of experiments varying bed diameter under these conditions:

25.7 ppm (117 mg/m^3) challenge concentration
50% relative humidity
(5.3-22)-m/min face velocities (20 L/min)
(3.4-6.9)-cm-diam x 2.5-cm-deep bed

These plots appear to be parabolic and, indeed, are best fit to quadradic equations for t_B (min) vs D (cm):

PF = 10, $t_B = 36.58\ D^2 - 69.51\ D - 98.60$, $r^2 = 0.969$
PF = 100, $t_B = 43.46\ D^2 - 251.15\ D + 377.40$, $r^2 = 0.996$
PF = 1000, $t_B = 48.73\ D^2 - 385.32\ D + 785.15$, $r^2 = 0.990$

Linear correlation coefficients r^2 of these equations were obtained by converting to the form $(T_B - a_0)/D$ vs D. As expected, breakthrough time increased greatly with bed diameter. Therefore, this is a very effective way of improving cartridge capacity and lifetime.

5. Bed Depth. This second bed dimension was also varied to observe the effects on t_B. Experimental conditions were:

25.7 ppm (117 mg/m^3) challenge concentration
50% relative humidity

14.7 m/min face velocity (30 L/min)
5.1-cm-diam x (1.25-5.0)-cm-deep bed

The t_B (min) vs bed depth d (cm) results plotted in Fig. 17 are most closely approximated by linear equations:

PF = 10, $t_B = -112.25 + 150.72d$, $r^2 = 0.998$
PF = 100, $t_B = -120.85 + 98.20d$, $r^2 = 0.990$
PF = 1000, $t_B = -147.24 + 74.62d$, $r^2 = 0.966$

At higher protection factors t_B vs d appears to deviate more from the linear relationship. A parabolic fit gives:

PF = 100, $t_B = -74.39 + 60.60d + 5.95d^2$, $r^2 = 0.924$
PF = 1000, $t_B = 63.70 - 48.86d + 16.46d^2$, $r^2 = 0.983$

A linear relationship of t_B vs d suggests that the breakthrough time was mainly determined by sorbent capacity in these experiments.

C. Discussion

1. **Breakthrough Curves.** Methyl iodide breakthrough curves of C_B/C_0 vs t were found to be best described by equations of the Theory of Statistical Moments. The more precise data over the widest range of C_B/C_0 required three statistical moments to fit the data. Having a mathematical description of this data is useful in two ways: (1) experimental data can be interpolated and extrapolated, and (2) physical meaning can be assigned to the statistical moments or combinations of them.

The usefulness of data smoothing and interpolation has been demonstrated in the calculation of t_B values for selected protection factors. These interpolated and extrapolated values were used in Figs. 10-17. Extrapolation of data to higher C_B/C_0 values up to 0.5 should be reliable. Beyond

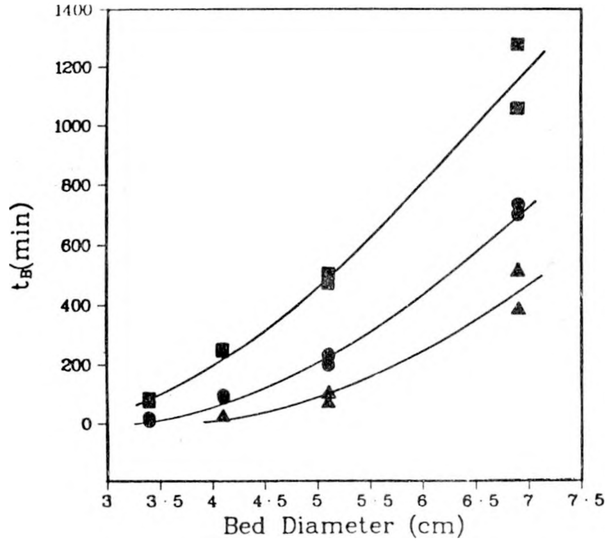

Fig. 16.
Bed diameter effects on breakthrough times for methyl iodide and 5% TEDA-impregnated Barnebey Cheney charcoal at protection factors: 10, ■ , and 100, ●, and 1000, ▲.

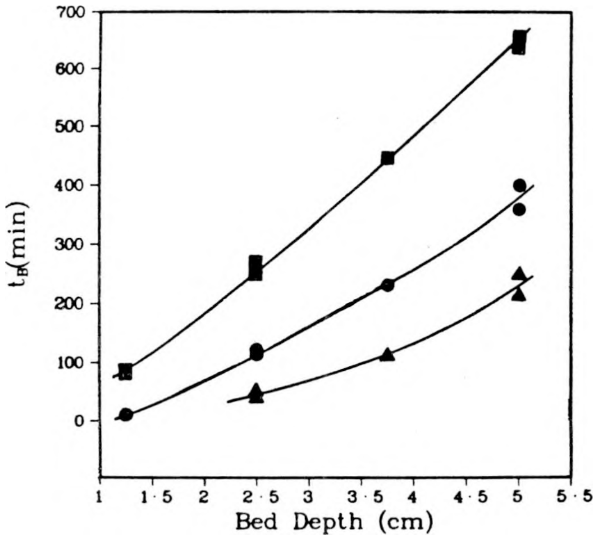

Fig. 17.
Bed depth effects on breakthrough times for methyl iodide and 5% TEDA-impregnated Barnebey Cheney charcoal at protection factors: 10, ■ , and 100, ●, and 1000, ▲.

0.5 there is no practical significance. However, extrapolation of C_B/C_o (or X_B) for t_B values smaller than experimental times (~4 min) is questionable. One reason is that the breakthrough concentration C_B measurements for the lower times of the range of data is near the limit of instrument detection. Here precision is usually least and here the deviation from linearity is greatest for t_B vs X_B plots such as in Figs. 7 and 9. Another reason for caution in extrapolating data to lower t_B values is that a finite bed depth allows a finite bed penetration at $t = 0$. This will be discussed in more detail below.

Another advantage of the use of the Theory of Statistical Moments is that the parameters obtained in fitting data can have physical significance. The first statistical moment, m_1 corresponds approximately to the mean of the breakthrough curve, where $C_B/C_o = 0.5$,

$$t_{0.5} = m_1 - \frac{m_3}{6m_2} \quad . \tag{5}$$

The second statistical moment, m_2 equals the variance (σ^2), which describes the spread of the breakthrough curve. And the third statistical moment, m_3, corresponds to the symmetry of the breakthrough curve. An effective adsorption bed capacity can be calculated as

$$F = 1 + \frac{\sqrt{m_2}}{m_1} (X_B) + \frac{m_3}{6m_1m_2} (X_B{}^2 - 1) \; . \tag{6}$$

A fractional bed capacity loss due to mass transfer is

$$M = -\frac{\sqrt{m_2}}{m_1} (X_B) - \frac{m_3}{6m_1m_2} (X_B{}^2 - 1) \; . \tag{7}$$

When appropriate assumptions are made, the parameters obtained by the Theory of Statistical Moments can be further related to measurable factors. For example, the assumption that mass transfer resistance is controlled by internal (pore) diffusion yields

$$\frac{\sqrt{m_2}}{m_1} = \left(\frac{2\, R^2\, V}{15\, \varepsilon D_i d}\right)^{\frac{1}{2}} \quad , \tag{8}$$

$$\frac{m_3}{6m_1m_2} = \left(\frac{R^2\, V}{21\, \varepsilon D_i d}\right) \quad , \tag{9}$$

where

R = adsorbent particle radius,
V = carrier gas face velocity,
d = bed length,
D_i = effective pore diffusion coefficient,
ϵ = internal/total porosity ratio.

Other adsorption mechanisms in which volumal adsorption and/or film mass transfer resistance are rate limiting yield similar relationships.[28] Experimental values of statistical moments can, therefore, suggest which mechanism is dominant. More practically, they can permit a cartridge designer or evaluator to predict t_B, F, and M as functions of flow velocity, bed dimensions, and sorbent properties. All three adsorption mechanisms predict that the fractional bed capacity loss M is a function of face velocity V(m/min): $M = a_1\sqrt{V} + b_1V$. The data of Fig. 15 for PF = 1000 fit this expression very well:

$$M = 0.494\sqrt{V} - 0.0655V,\ r^2 = 0.939. \tag{10}$$

Likewise, M should be a function of bed depth d (cm); $M = a_2/L + b_2/\sqrt{L}$. The data of Fig. 17 for PF = 1000 fit this expression very well:

$$M = -1.748/L + 2.558/\sqrt{L},\ r^2 = 0.990. \tag{11}$$

2. Challenge Concentration Effects. Most of the data available on respirator cartridge service lives have been obtained in the parts-per-million to parts-per-thousand concentration range. For example, Gary Nelson and coworkers at the Lawrence Livermore Laboratory measured service lives for 131 organic vapors.[30] These were obtained mostly at 1000 ppm challenge concentration with a few measurements as low as 50 ppm.[31] Yet, the acceptable levels for many toxic compounds are well below 1000 ppm. The experimental lower limit for time-resolved breakthrough measurements is about 1-ppm challenge or 10-ppb breakthrough concentration. Carcinogenic compounds and radionuclides in air will occur below the 1-ppm level, except in very unusual and dangerous circumstances. Respirator cartridge service life data can be obtained easily at parts-per-million concentrations. Can this data be extrapolated to describe the performance of an identical cartridge at lower concentrations?

How is the service lifetime of an adsorbent bed affected by concentration of the air drawn through it? An apparent answer is that an adsorbent bed has a fixed capacity; therefore, the service life is inversely proportional to the challenge concentration. Double the concentration and reduce the lifetime by half. A more thoughtful answer may be this: At low vapor concentrations the adsorption isotherm should be Henry's Law; in other words, capacity is proportional to vapor concentration. Therefore, the service life is independent of challenge vapor concentration. As is often the case, the correct answer lies between these two extremes: the capacity and, therefore, the service life varies with concentration, but not necessarily inversely.

In 1969 Fraust and Hermann published a report on the adsorption of aliphatic acetate vapors on activated charcoal.[32] They observed that log-log plots of breakthrough times vs challenge concentration were linear at 10% and 50% breakthrough fraction. Nelson and Harder observed the same relationships for methyl acetate, acetone, and eight other vapors.[31] The log-log plots for a wide range of per cent breakthrough were linear and parallel. In our studies with methyl iodide and an activated charcoal we also observed an apparently linear relationship on a log breakthrough time vs log challenge concentration plot (Fig. 12). Methyl iodide adsorbed on a TEDA-impregnated charcoal also gave similar results, but with larger negative slopes (Fig. 13). These relationships can be summarized by the empirical equation,

$$t_B = a_B C_o^{-b_B}. \tag{12}$$

The subscript, capital B, refers to a given breakthrough fraction. Values of b_B, the negative slopes of the log-log plots that have been observed, are given in Table VII. These values vary widely from 0.27 to within experimental uncertainty of one.

The empirical equation for breakthrough time or service life can be transformed into an adsorption isotherm equation by multiplying by volumetric flow rate (w) and challenge concentration (C_o). Figure 18 shows dynamic adsorption isotherms at three breakthrough fractions for methyl iodide and activated charcoal. These isotherms were calculated from experimental breakthrough curves. Capacity is neither constant nor proportional to challenge concentration. It is dependent on the breakthrough fraction you will allow.

The empirical equation for dynamic adsorption isotherms is given by

$$\begin{gathered} V_B = w\ C_o\ t_B = w\ a_B\ C_o^{\ 1-b_B} \\ 0.27 \le b_B \le 1.0 \\ 0 \le 1-b_B \le 0.83 \quad . \end{gathered} \tag{13}$$

The exponential form and the experimental range of b_B, between 0.27 and one, are consistent with the classical (Freundlich) adsorption isotherm:

$$\begin{gathered} V = k\ p^{1/n} \\ n \ge 1,\ 0 < 1/n \le 1 \quad . \end{gathered} \tag{14}$$

The experimental values of ($1-b_B$) fall within the 0 to 1 range of 1/n and the empirical isotherm has the same concentration (pressure) dependence as the classical isotherm. Therefore, the identification of $1-b_B$ with 1/n is possible.

What is the significance of this identification? First, the classical isotherm equation has been derived assuming that heat of adsorption decreases exponentially with surface coverage by the adsorbate.[33] Therefore, a similar exponential variation of activity of surface adsorption sites should be the determining factor for observed service life dependence on challenge concentration. It is also unlikely that the exponential variation in heat of adsorption, reflected in the exponent

TABLE VII

CONCENTRATION DEPENDENCE PARAMETERS FOR BREAKTHROUGH TIMES

Researchers	Vapors	Concentration Range	b_B Values For Breakthrough Fractions B=0.1	b_B Values For Breakthrough Fractions B=0.5
Fraust and Hermann[a]	4 Acetates	100-1000 ppm	1.004-1.072	0.974
Nelson and Harder[b]	10 Organics	50-3000 ppm	0.348-0.937	
Wood, et al.[c]	Methyl Iodide	10-1000 ppm	0.27 ± 0.08	0.35 ± 0.05
	Methyl Iodide[d]	1-29 ppm	1.01 ± 0.03	1.06 ± 0.06
	Iodine	8-32 ppm	0.83 ± 0.30	0.87 ± 0.41

---

[a] Ref. 32.

[b] Ref. 31.

[c] This report and other unpublished results.

[d] 5% Triethylenediamine impregnated charcoal.

1/n, will continue unchanged to concentrations much lower than the experimental data. An adsorbent such as activated charcoal, in particular, is certain to have a wide range of adsorption site types and activities. Therefore, quantitative extrapolation of breakthrough times or capacities to much lower concentrations is very questionable.

However, the breakthrough times measured at parts-per-million concentrations do have some value for applications at lower challenge concentrations. This simple calculation shows that breakthrough time is proportional to the slope of the corresponding adsorption isotherm at any challenge concentration.

$$\begin{aligned} t_B &= a_B\ C_o^{\ -b_B} \\ V_B &= w\ a_B\ C_o^{\ 1-b_B} \\ dV_B/dC_o &= (1-b_B)\ w\ a_B\ C_o^{\ -b_B} \\ &= (1-b_B)\ w\ t_B \ . \end{aligned} \tag{15}$$

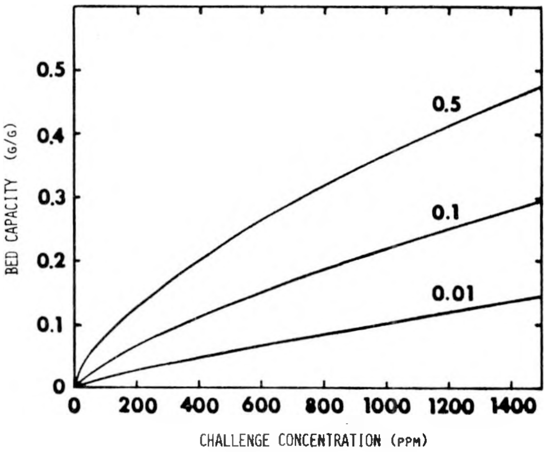

Fig. 18.
Dynamic adsorption isotherms for methyl iodide and nonimpregnated Union Carbide ACC charcoal at three breakthrough fractions, 50% relative humidity, 9.8 m/min (20 L/min) airflow rate, and 5.1-cm-diam by 2.5-cm-deep bed.

The slope of the classical isotherm increases with decreasing vapor concentration (Fig. 18); therefore, the breakthrough time increases with decreasing concentration. Even if the exponent of the classical adsorption isotherm changes, the isotherm will always be either concave to the concentration axis or linear. Only for multilayer adsorption at high vapor concentrations can the isotherm curve upwards. Therefore, in all realistic situations a service life measured at a parts-per-million challenge concentration will be a lower limit of the service life at any lower concentration.

In summary, from this analysis we have concluded that:

(1) The challenge concentration dependence of breakthrough times at ppm levels conforms to the nonlinear classical adsorption isotherm equation.

(2) Quantitative extrapolation of concentration effects to much lower concentrations is questionable since parameters dependent on surface activities may change.

(3) Breakthrough time is proportional to the slope of the corresponding adsorption isotherm, and this slope increases or is unchanged at lower concentrations.

(4) Therefore, service lives of adsorbent cartridges determined at ppm levels are lower limits to service lives for lower concentrations.

VI. PROJECT STATUS

By the end of this reporting period, we have accomplished the first three steps towards our goal listed in Sec. II above. An examination of the available and relevant literature and contacts with professionals knowledgeable in air cleaning and respirator applications were made. We have concluded that an air-purifying respirator cartridge or canister with high efficiency (PF = 1000) for vapor forms of radioiodine is feasible. However, there are some critical parameters that affect sorbent cartridge performance: type of sorbent, bed geometry, work load (breathing rate) of the user, relative humidity, history of use, and form of airborne radioiodine. Cartridge or canister contents and design will be determined by the manufacturers. The test method must include extreme relative humidity and airflow rate appropriate to each design. Cartridge history must be controlled by use practices and bookkeeping. The most penetrating form of radioiodine is probably methyl iodide, and this should be the major test species.

Development and study of suitable testing equipment was started. A flow system was designed and built for testing efficiencies and capacities of sorbent beds using stable ^{127}I vapor species. Control and variation of critical parameters were built into the system. Methyl iodide concentrations of 1-1000 ppm could be generated. Detection was primarily by a gas chromatograph with an electron capture detector. Elemental iodine could also be generated.

Experimental studies challenged potential respirator sorbents with methyl iodide vapor. The first objective was to find a mathematical model to describe the breakthrough of vapor through such beds. A set of equations of the Statistical Moments Theory best described breakthrough curves. This model subsequently proved to be a powerful tool for data analysis. The second objective was to confirm the magnitudes of effects of variables such as airflow rate, relative humidity, vapor concentration, and bed geometry. Measurements of these effects under limited conditions have been quite useful in understanding the limitations of various sorbents and in understanding how to identify these limitations.

Future steps toward the ultimate goal of a respirator cartridge (or canister) testing criteria and procedure have been listed previously (Sec. II). We are progressing steadily toward that goal close to the schedule originally proposed. Apparatus development will proceed in parallel to and closely tied to experimental studies of adsorption and retention of iodine vapor species. Test techniques and apparatus and experimental results will be shared with NIOSH, NRC, and other interested parties as they are developed in this project.

REFERENCES

1. E. C. Hyatt, "Respirator Protection Factors," Los Alamos Scientific Laboratory report LA-6084-MS (January 1976).

2. "Acceptable Programs for Respiratory Protection," Regulatory Guide 8.15, U. S. Nuclear Regulatory Commission (October 1976).

3. J. L. Caplin, B. J. Held, R. J. Catlin, "Manual of Respiratory Protection Against Airborne Radioactive Materials," NUREGL=0041, U.S. Nuclear Regulatory Commission (1976). Available from the National Technical Information Service, Springfield, Virginia 22161.

4. K. Boddy, R. F. Mathams, and F. H. Weller, "Calculation of Tellurium and Iodine Fission Product Activities," Nucleonics **22**, 130 (1964).

5. J. O. Blomeke and J. J. Perona, "Soource Terms for Airborne Effluents," CONF-760806-5 (1976).

6. C. A. Pelletier, J. E. Cline, and J. H. Keller, "Measurement of Sources of Iodine-131 Releases to the Atmosphere from Nuclear Power Plants," IEEE Trans. Nucl. Sci. **21**, 478 (1974).

7. A.E.J. Eggleton and D. H. Atkins, "Identification of Radioiodine Compounds Formed on Releasing Carrier-Free Iodine-131 in Air," Amer. Nucl. Soc. Trans. **6**, 129 (1963).

8. R. Vilenchick and J. W. Hodgins, "Gamma Initiated Iodination of Methane in the Gas Phase," Can. J. Chem. Eng. **48**, 588 (1970).

9. J. L. Kovach, "Evaluation of Currently Available Data for Low Concentration Iodine Fission Product Removal," NUCON 078, Nuclear Consulting Services, Inc., Columbus, Ohio (1974).

10. U. S. Atomic Energy Commission, "USAEC Rules and Regulations, Title 10, Code of Federal Regulations, Part 20, Standards of Protection Against Radiation," Revised (August 9, 1966).

11. L. Silverman, G. Lee, T. Platkin, L. A. Sawyers, A. R. Yancey, "Air Flow Measurements on Human Subjects With and Without Respiratory Resistance at Several Work Rates," A.M.A. Arch. Ind. Hyg. J. **3**, 461 (1951).

12. G. O. Nelson and C. A. Harder, "Respirator Cartridge Efficiency Studies IV. Effects of Steady-State and Pulsating Flow," Amer. Ind. Hyg. Assoc. J. **33**, 797 (1974).

13. R. R. Bellamy, "Elemental Iodine and Methyl Iodide Adsorption on Activated Charcoal at Low Concentrations," Nucl. Safety **15**, 711 (1974).

14. R. L. Ritzman and J. M. Genco, "Evaluation of Data Regarding the Efficiency of Activated Charcoal Adsorbers at Low Gas Phase Iodine Concentration," U.S. Atomic Energy Commission report WASH-1231 (1972).

15. D. S. Deshingkar, K. Ramarathinam, and A. A. Khan, "Selection of Suitable Activated Charcoals for Iodine Filters," Government of India Atomic Energy Commission report BARC-765 (1974).

16. R. E. Adams and W. E. Browning, Jr., "Iodine Vapor Adsorption Studies for the NS 'Savanna' Project," Oakridge National Laboratory report ORNL-3726 (February 1965).

17. R. E. Adams and R. D. Ackley, "Removal of Elemental Radioiodine from Flowing Humid Air by Iodized Charcoals," U.S. Atomic Energy Commission report ORNL-TM-2040 (November 1967).

18. R. E. Adams, R. D. Ackley, and Z. Combs, "Trapping Radioactive Iodine and Methyl Iodide by Impregnated Charcoals," U.S. Atomic Energy Commission report ORNL-4374 (June 1969).

19. D. T. Pence, F. A. Duce, and W. J. Maeck, "Developments in the Removal of Airborne Iodine Species with Metal Substituted Zeolites," Proceedings of the 12th AEC Air Cleaning Conference, CONF-720823 (1972).

20. D. A. Collins, L. R. Taylor, and R. Taylor, "The Development of Impregnated Charcoals for Trapping Methyl Iodide at High Humidity," United Kingdom Atomic Energy Authority TRG report 982 (W) (1965).

21. F. G. May and H. J. Polson, "Methyl Iodide Penetration of Charcoal Beds: Variation with Relative Humidity and Face Velocity," Australian Atomic Energy Commission report AAEC/E322 (September 1974).

22. J. L. Kovach and J. R. Hunt, "Iodine Fission Product Mass Transfer in Adsorbent Media," Proceedings of the 13th AEC Air Cleaning Conference, CONF-740807 (August 1974).

23. V. R. Deity, C. H. Blachly, and L. A. Jonas, "Dependence of Gas Penetration of Charcoal Beds on Residence Time and Linear Velocity," Proceedings of the 14th ERDA Air Cleaning Conference, CONF-760822 (February 1977).

24. W. J. Maeck, D. T. Pence, and J. H. Keller, "A Highly Efficient Inorganic Adsorber for Airborne Iodine Species (Silver Zeolite Development Studies)," Proceedings of the 10th AEC Air Cleaning Conference, CONF-680821 (December 1969).

25. D. T. Pence, F. A. Duce, and W. J. Maeck, "A Study of the Adsorption Properties of Metal Zeolites for Airborne Iodine Species," Proceedings of the 11th AEC Air Cleaning Conference, CONF-700816 (December 1970).

26. M. J. Kabat, "Testing and Evaluation of Adsorbers for Gaseous Penetrative Forms of Radioiodine," Proceedings of the 13th AEC Air Cleaning Conference, CONF-740807 (March 1975).

27. Science Applications, Inc., Nuclear Environmental Services Division, "Testing Results of Respirator Cartridges for Protection Against Radioiodine Vapors," a report for the Vermont Yankee Nuclear Power Station (February 1977).

28. O. Grubner and D. W. Underhill, "Calculation of Bed Capacity by the Theory of Statistical Moments," Separation Science **5**, 555 (1970).

29. O. Grubner and W. A. Burgess, "Simplified Description of Adsorption Breakthrough Curves in Air Cleaning and Sampling Devices," Am. Ind. Hyg. Assoc. J. **40**, 169 (1979).

30. G. O. Nelson and C. A. Harder, "Respirator Cartridge Efficiency Studies: V. Effects of Solvent Vapor," Am. Ind. Hyg. Assoc. J. **35**, 391 (1974).

31. G. O. Nelson and C. A. Harder, "Respirator Cartridge Efficiency Studies: VI. Effect of Concentration," Am. Ind. Hyg. Assoc. J. **37**, 205 (1976).

32. C. L. Fraust and E. R. Hermann, "The Adsorption of Aliphatic Acetate Vapors onto Activated Carbon," Am. Ind. Hyg. Assoc. J. **30**, 494 (1969).

33. J. Zeldowitsch, "Theory of the Freundlich Adsorption Isotherm," Acta Physiocochim. U.R.S.S. **1**, 961 (1934), (Chem. Abs. **29**, 6485-5).

DISTRIBUTION

	Copies
Nuclear Regulatory Commission, RH	148
Technical Information Center, Oak Ridge, Tennessee	2
Los Alamos Scientific Laboratory	50
	200